

Finding Free Surface of Supercritical Flows - Numerical Investigation

Robert Feurich & Nils Reidar B. Olsen

To cite this article: Robert Feurich & Nils Reidar B. Olsen (2012) Finding Free Surface of Supercritical Flows - Numerical Investigation, Engineering Applications of Computational Fluid Mechanics, 6:2, 307-315, DOI: [10.1080/19942060.2012.11015423](https://doi.org/10.1080/19942060.2012.11015423)

To link to this article: <https://doi.org/10.1080/19942060.2012.11015423>



Copyright 2012 Taylor and Francis Group
LLC



Published online: 19 Nov 2014.



Submit your article to this journal [↗](#)



Article views: 328



View related articles [↗](#)

FINDING FREE SURFACE OF SUPERCRITICAL FLOWS - NUMERICAL INVESTIGATION

Robert Feurich * and Nils Reidar B. Olsen

Department of Hydraulic and Environmental Engineering, The Norwegian University of Science and Technology, S.P. Andersens veg 5, 7491 Trondheim, Norway

** E-Mail: robert.feurich@ntnu.no (Corresponding Author)*

ABSTRACT: A three-dimensional numerical model (STAR-CCM+) has been used to compute the free surface for different cases with supercritical flow. The program solves the Navier-Stokes equations on an unstructured hexahedral grid using the SIMPLE method and the k-epsilon turbulence model. The location of the free water surface has been computed with the volume of fluid method. Two cases from literature have been used for validation: one with a channel expansion and another with a channel junction. In both cases, oblique standing waves occurred. The geometry of the waves were well reproduced by the numerical model. The third case had a more complex geometry, modelling a physical laboratory study of a natural river geometry upstream of the dam of a hydropower plant. The case was unusual in that supercritical flow and oblique standing waves occurred upstream of the dam. Also for this case the numerical model gave reasonable results for the location of the free water surface.

Keywords: supercritical flow, physical model, numerical model, volume of fluid (VOF) method, free surface flow

1. INTRODUCTION

Supercritical flows often appear in spillway channels, chutes and other man-made hydraulic structures. Knowledge of the increased free surface elevation due to supercritical flows is of immense importance especially in case of changing cross section geometries, friction, slope or small obstacles within the flow area. The resulting standing water waves are also called shock-waves and can cause damage to hydraulic structures and the surrounding environment unless they are considered during construction phase.

One way of assessing the effects of supercritical flows on water levels is by physical model tests investigating different flow and geometry setups. Empirical formulas, such as deflection angles or height of the shock front, can also be found (Ippen and Knapp, 1936; Ippen and Dawson, 1951; Rouse et al., 1951; Bowers, 1950; Hager, 1989; Mazumder and Hager, 1993).

Computational fluid dynamics (CFD) has almost completely replaced experimental investigations in areas like mechanical or aerospace engineering. The techniques have also become popular and reliable in hydraulic engineering over the last years. However, the use of numerical models in this field has much been restricted to one (1D) or two dimensional (2D) computations. CFD has also been used to calculate supercritical flows, mainly using 2D depth-averaged approaches (e. g.

Jimenez and Chaudhry, 1988; Soulis, 1991; Krüger and Rutschmann, 2006; Mignot et al., 2008; Ying et al., 2009). Haun et al. (2011) used a width-averaged approach to model a broad-crested weir. Despite the fact that the results of the 2D simulations were quite reasonable, the flow situation of supercritical flows with oblique shockwaves is in fact a complex three dimensional (3D) problem. Stamou (2008) applied the commercial 3D numerical model Flow-3D from Flow Science to successfully simulate the expansion channel by Mazumder and Hager (1993) using the Volume of Fluid (VOF) approach to track the free surface. Hargraeves et al. (2007) validated the VOF model for FLUENT 6.2 from Fluent Inc. simulating the free surface flow over a broad crested weir in 2D and 3D.

In the current study we validate a numerical model (STAR-CCM+) on two simpler cases before applying it to a more complex geometry from a physical model of a river/spillway.

The algorithms to find the position of the free water surface are a particular challenge. First tests using a 3D approach were performed using a simplified potential flow approach as described in Chan and Larock (1973) and Chan et al. (1973). First results using the Navier-Stokes equations were obtained using the marker and cell (MAC) method (Harlow and Welch 1965). Later this method was improved using on a fixed mesh either the VOF method (Hirt and Nichols 1981) or the level set method described in Sethian (1996)

which are somewhat similar. Mnasri et al. (2010) successfully used the VOF method in 2D for simulating the free surface behaviour when horizontal cylinders are exiting and entering. Zhou et al. (2011) applied the VOF model to transients in water filling pipes containing entrapped air pockets using 2D and 3D simulations. An alternative way in the finite element community was chosen by Hughes et al. (1981) or Huerta und Liu (1988) using space-time finite elements and the ALE (Arbitrary Lagrangian-Eulerian) method. Flow in spillway structures has been computed by e.g. Olsen and Kjellesvig (1998), Bürgisser (1998) and Bürgisser and Rutschmann (1999). An interesting approach is presented in Krüger et al. (1998) and Krüger (2000) who derived the extended shallow water equations proving 3D flow features on a 2D computational mesh.

In cases where air entrainment can occur, which is highly possible for supercritical flows, prototype data should be preferred over laboratory data for testing the numerical models.

One of the advantages of numerical modelling is the time and money saving aspect compared to physical model studies. Chandler et al. (2003) and Gessler and Rasmussen (2005) reported that the costs are reduced to 20 - 25% and the time to 25 - 33%.

2. NUMERICAL MODEL

The supercritical flow configurations in the current study are characterized by a strong three-dimensional structure and a free water surface including standing waves. Therefore the 3D simulation tool STAR-CCM+ was chosen because it can handle complex three dimensional flow situations and by using the volume of fluid (VOF) method every kind of free water surface can be reproduced. STAR-CCM+ is a multipurpose computational fluid dynamics (CFD) software produced by CD-adapco (2010). STAR-CCM+'s numerical solver is based on the finite volume method (FVM) and handles structured and unstructured grids. Different mesh types are available in the software. When investigating the free surface flow, the hexahedral (trimmed) mesh was found optimum because the grid lines are more aligned with the flow direction, causing less false diffusion. This results in a smoother water surface compared to tests with polyhedral and tetrahedral meshes.

2.1 Basic theory

The program solves the Reynolds-Averaged Navier-Stokes (RANS) equations (continuity Eq. 1 and momentum Eq. 2).

$$\frac{\partial U_i}{\partial x_i} = 0 \quad (1)$$

$$\frac{\partial U_i}{\partial t} + \frac{\partial}{\partial x_j} (U_i U_j + \overline{u_i u_j}) = \frac{1}{\rho} \left(-\frac{\partial P}{\partial x_i} + \frac{\partial \overline{\tau_{ij}}}{\partial x_j} \right) + G_i \quad (2)$$

with $i, j = 1, 2, 3$

where U_i is the velocity averaged over time t in the subscript direction, u_i is the velocity fluctuation over time, x is the spatial geometrical scale, ρ is the water density, P is the pressure, G_i is the gravitational force and $\overline{\tau_{ij}}$ represents the components of the mean viscous stress term.

$$\overline{\tau_{ij}} = \mu \left(\frac{\partial U_i}{\partial x_j} + \frac{\partial U_j}{\partial x_i} \right) \quad (3)$$

The equations are obtained by decomposing the Navier-Stokes equations into a mean and fluctuating component which results in a term \mathbf{T}_t , known as the Reynolds stress tensor as follows (CD-Adapco, 2010).

$$\mathbf{T}_t \equiv -\overline{\rho u_i u_j} \quad (4)$$

The Reynolds stresses have to be estimated by a turbulence model to solve the equations above. In this study the $k-\varepsilon$ model, an eddy viscosity model, has been used. The basic principle of that approach is to introduce a turbulent viscosity μ_t , to model the Reynolds stress tensor using mean velocities (Ferziger and Perić, 2002).

$$-\overline{\rho u_i u_j} = \mu_t \left(\frac{\partial U_i}{\partial x_j} + \frac{\partial U_j}{\partial x_i} \right) - \frac{2}{3} \rho \delta_{ij} k \quad (5)$$

where k is the turbulent kinetic energy given below and δ_{ij} is Kronecker delta

$$k = \frac{1}{2} \overline{u_i u_i} = \frac{1}{2} (\overline{u_x u_x} + \overline{u_y u_y} + \overline{u_z u_z}) \quad (6)$$

The transport equations for k and its dissipation rate ε are as follows

$$\rho \frac{\partial k}{\partial t} + \rho U_j \frac{\partial k}{\partial x_j} = \frac{\partial}{\partial x_j} \left[\left(\mu + \frac{\mu_t}{\sigma_k} \right) \frac{\partial k}{\partial x_j} \right] + P_k - \rho \varepsilon \quad (7)$$

$$\rho \frac{\partial \varepsilon}{\partial t} + \rho U_j \frac{\partial \varepsilon}{\partial x_j} = \frac{\partial}{\partial x_j} \left[\left(\mu + \frac{\mu_t}{\sigma_\varepsilon} \right) \frac{\partial \varepsilon}{\partial x_j} \right] + C_{\varepsilon 1} \frac{\varepsilon}{k} P_k - \rho C_{\varepsilon 2} \frac{\varepsilon^2}{k} \quad (8)$$

in which μ is molecular viscosity and P_k defined as follows

$$P_k = \mu_t \left(\frac{\partial U_i}{\partial x_j} \frac{\partial U_i}{\partial x_j} + \frac{\partial U_j}{\partial x_i} \right) \quad (9)$$

The turbulent viscosity can then be calculated as

$$\mu_t = \rho C_\mu \frac{k^2}{\varepsilon} \quad (10)$$

The most common values for the five parameters of that model are (Ferziger and Perić 2002).

$$\begin{aligned} C_\mu &= 0.09 & C_{\varepsilon 1} &= 1.44 & C_{\varepsilon 2} &= 1.92 \\ \sigma_k &= 1.0 & \sigma_\varepsilon &= 1.3 \end{aligned} \quad (11)$$

2.2 Free surface tracking

Usually, the flow through hydraulic structures is characterized by a free water surface. The position of this surface is not known a priori and therefore the application of a numerical tool is not trivial. Because the free surface boundary of the domain for the computation can not be defined a priori, the discretization into computational cells is not straightforward. For 3D computations the solution procedure strategies can be as follows:

- Using a flexible mesh which iteratively adapts to the correct position of the free surface.
- Working with a fixed mesh using additional information on the content of flow in each cell.

The first approach is implemented in the ALE (Arbitrary Lagrangian-Eulerian) concept used mainly in a finite element context. The second strategy was successfully applied both in the MAC (marker and cell) method and in the VOF (volume of fluid) approach proposed by Harlow and Welch (1965) and Hirt and Nichols (1981) respectively. The latter is implemented in the software used for the present investigation.

The principle of the VOF method is to use additional scalar information in each cell to track the ratio of water and air within the whole domain. The exact position where the free surface cuts through a cell ($0 < f < 1$) is determined using the scalar (f) information in the cell itself and its neighbouring cells. Similarly, the normal vector

on the plane can be determined. An additional transport equation has to be solved for f .

$$\frac{\partial f}{\partial t} + U_i \frac{\partial f}{\partial x_i} = 0 \quad (12)$$

3. VERIFICATION OF MODEL

For testing the reliability of the numerical model when simulating flows with high Froude numbers correctly, results of two experimental test cases from literature have been chosen. One case is investigating the supercritical flow in an expansion with a Rouse-modified transition geometry (Mazumder and Hager, 1993). The other is dealing with the supercritical flow in a channel junction (Hager, 1989).

3.1 Test case 1 – expansion

The first test case was the physical model study by Mazumder and Hager (1993). Figure 1 shows the geometry and the dimensions of the horizontal channel expansion.

For the evaluation of the numerical model one case with an approach Froude number $F_0 = 8.0$ at the inflow boundary has been chosen. The 2.0 m long modified Rouse boundary curve $y_b(x)$ was defined as follows

$$\frac{y_b}{b_0} = \frac{1}{2} \left(1 + \frac{1}{4} X^{3/2} \right) \quad (13)$$

where

$$X = x / (b_0 F_D) \quad (14)$$

b_0 is the channel width at inflow; the design Froude number (F_D) equals 1.

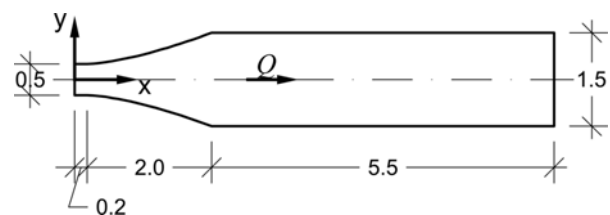


Fig. 1 Plan view of channel expansion geometry [m].

3.2 Test case 1 - numerical setup

A trimmed mesh consisting of hexahedral cells has been chosen for stability purposes of the numerical simulation. The mesh used 2.2 million cells and Dirichlet boundary conditions at the boundaries. Due to the low water depths at the corners at the end of the channel expansion a grid refinement had to be used there. Figure 2 shows the grid at the end of the expansion with the

refinements in the main water flow area and the edges.

To reduce instabilities at the beginning of the simulation the domain has been filled with water up to the water height ($h_0 = 0.048$ m) of the inflow boundary and a mean velocity (5.5 m/s) has been given to that water body. A time step of 0.003 seconds has been applied.

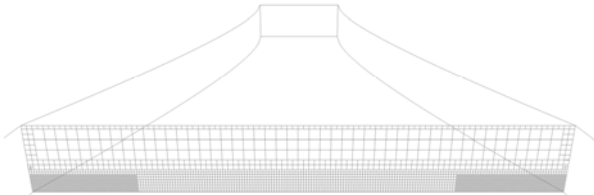


Fig. 2 Grid refinement at end of expansion, looking upstream.

3.3 Test case 1 – results

Figure 3 shows the comparison of the measured (a) and calculated (b) results. The free surface elevation (h) is presented in relation to the inflow water height (h_0). It can be clearly seen that the numerical results fit very well with the measurement data. For example the small area of shallow flow at the wall, directly upstream the edge of the expansion ending, has been reproduced by the numerical model. Also the location and shape of the wave front starting in the edge at the end of the channel expansion has been reproduced well by the numerical simulation.

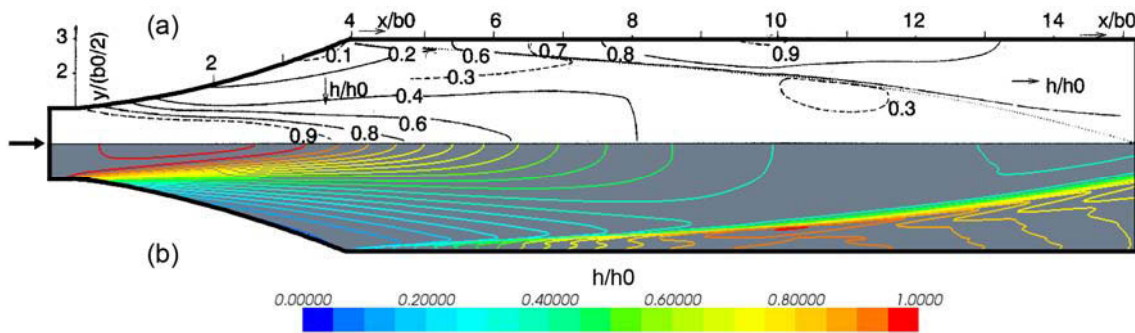


Fig. 3 Comparison of computed free surface elevation with measurement (Krüger and Rutschmann, 2006): (a) Experimental data; (b) Simulation results.

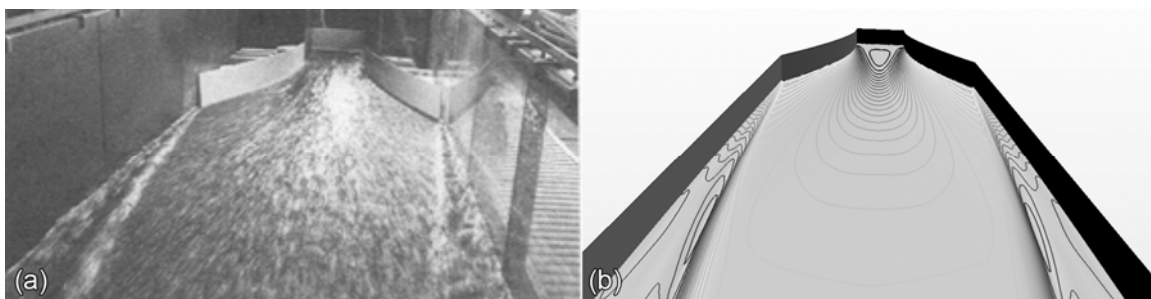


Fig. 4 Free surface comparison: (a) Physical model (Mazumder and Hager, 1993); (b) Simulation.

The only obvious difference is the smoothness of the contour lines between the wave front and the channel walls, but the values are still within the same range.

A qualitative comparison between simulation and measurement is given in Figure 4. Also here the good agreement between simulation and measurement can be clearly seen. The wave front on both sides of the channel downstream of the expansion as well as the water surface within the expansion fit very well between measurement and simulation.

3.4 Test case 2 – channel junction

A small channel junction experimentally investigated for different flow situations by Hager (1989) has been used as second test case for the numerical model (Fig. 5). In the chosen test case the upstream Froude number (F_0) is 4.5 in both branches, which are connected by an angle (δ) of 22.5° . The total length is 0.6 m with a channel width of 0.1 m.

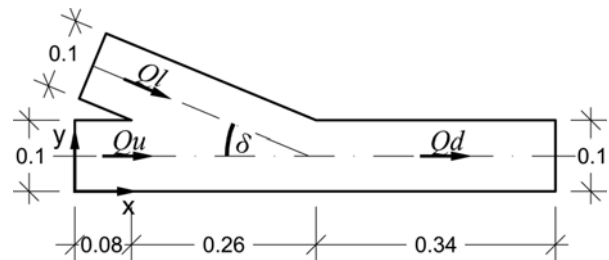


Fig. 5 Plan view of channel junction geometry [m].

3.5 Test case 2 - numerical setup

Similar to the first test case, a trimmed mesh with Dirichlet boundary condition was used. In this case 1.3 million cells and a time step of 0.001 s were necessary to obtain reliable results. As for the expansion case, the domain was filled with water up to the inflow boundary water depth ($h = 0.0268$ m) as initial condition.

3.6 Test case 2 – results

Figure 6 shows the contour lines of the free surface elevation from measurement and simulation.

The shape, angle and location of the wave front within the channel junction show a very good agreement between measurement and simulation. The overall pattern of the two results fits quite well, although the maximum water height at the right side of the channel, downstream the junction, is too low. However, the height is in the same range as the results of Krüger and Rutschmann (2006) using an extended shallow water approach. The three dimensional code used in the current study improved the results compared to Krüger and Rutschmann (2006) on the left side of the channel, which fits quite well in the present study. When looking at the water surface in the middle of the channel, just upstream of the channel outflow, it can be seen that the elevation and the shape are matching well.

One reason for the difference in the maximum water surface elevation might be that air entrainment has not been considered in the numerical simulation. The high Froude numbers of the flow make air entrainment highly possible in the area.

When looking at the 3D-shape of the free surface in the junction area (Figure 7) it can also clearly be seen that the numerical simulation is representing the flow situation reasonably well.

4. APPLICATION OF THE MODEL

The numerical model validated with the two test cases in the previous section has been used to investigate the free surface of the highly complex three dimensional flow situation upstream of the weirs of the Sarpfossen hydropower dam in Norway. The power plant is located at the end of the largest Norwegian river, Glomma. The Sarpfossen (also Sarpefossen) waterfall has become a landmark of the city Sarpsborg which is located approximately 73 km southeast of Oslo (Norway). Three hydropower plants are installed in that area with more than 142 MW of

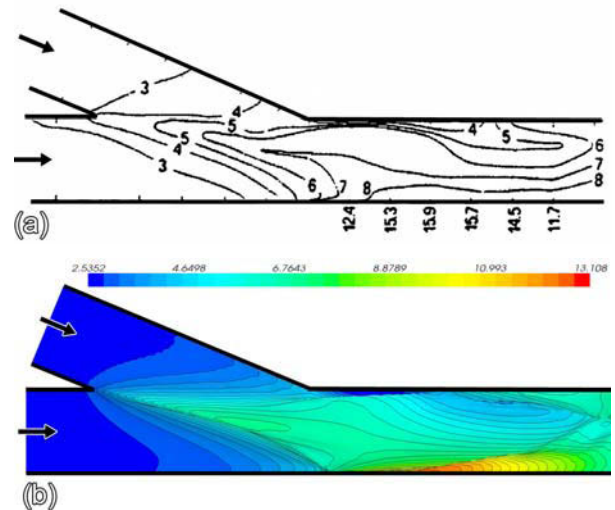


Fig. 6 Free surface elevation [cm]: (a) Measurement (Hager, 1989); (b) Simulation.

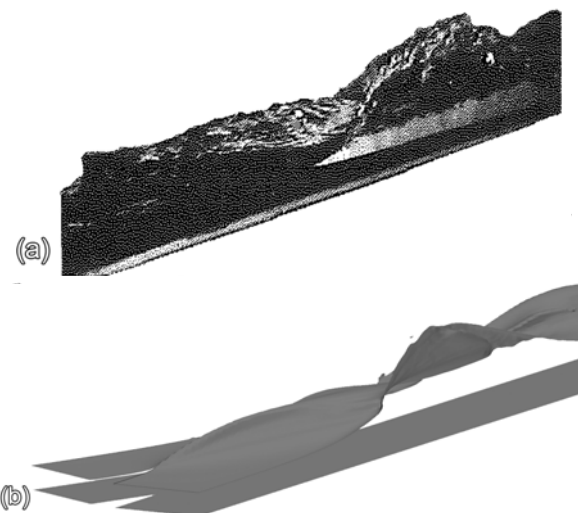


Fig. 7 Free surface comparison, flow from left to right: (a) Physical model (Hager, 1989); (b) Simulation.

production capacity (Sarp power plant, Hafslund power plant to the east and Borregaard power plant on the west side of the waterfall).

4.1 Physical model study

The physical model of the Sarpfossen hydraulic structure was built in the hydraulic laboratory of the Norwegian University of Science and Technology (NTNU) in Trondheim (Figure 8) to assess the hydraulic conditions for the maximum probable flood ($6000 \text{ m}^3/\text{s}$). The model consists of the Sarpfossen dam, weirs and the river area upstream of the dam. The modelled area of approximately 1000×600 m in nature corresponds to 22×13 m in model scale (1:45). The main purpose of the model study was to investigate the effect of the reduced cross-section

area, caused by the bridge piers, on the capacity of the spillway.

On the spillway crest three gates were installed - two flap gates and a sector gate. The sector gate in the Sarpfossen dam has a width of 27.9 m, height of approximately 7.5 m and radius of 10.8 m. The flap gates are located on the right side, in flow direction, and both are about 5 m in height. Furthermore, each flap gate has a span length of approximately 13.5 m.

The test runs used for this study have been conducted with a flow rate of 3396 m³/s (250 l/s in model) due to a flood event in 1995 with that discharge. During the testing, all power plant intakes were closed and the spillway gates were open completely. The water levels between the weirs and the bridge upstream were measured using a horizontal laser beam giving a determined height level as a fixed reference value and a ruler to measure the distance between that beam and the water level. Approximately 24 points along each cross section were taken.

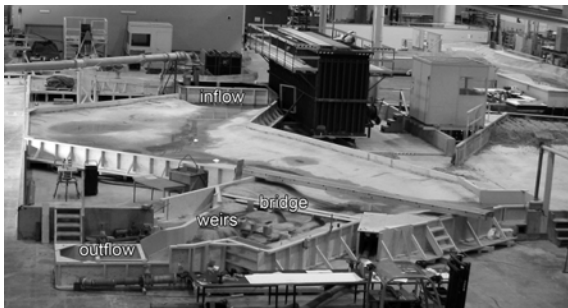


Fig. 8 Physical model in NTNU hydraulic laboratory.

4.2 Numerical setup

The flow volume with the riverbed as bottom wall boundary was imported to STAR-CCM+ using a stereolithography (STL) file, where the solid object surface is represented by triangles. Figure 9 shows the project area and the cross-sections used for modelling the geometry.

The intakes of the power plants have not been considered in the numerical model because they were also closed in the physical model test. Besides the wall boundaries, a velocity inlet boundary was used for the fluid fraction at the first cross-section. A symmetry boundary was used at the top and a pressure outlet boundary downstream of the weirs was used to get rid of the water without affecting the upstream flow as in the physical model. The top boundary was placed approximately 1 m above the free water surface to minimize the effect of the air flow on the free surface. For the bottom boundary a roughness height of 2 mm was defined, which corresponds to the roughness of a good-quality concrete.

The domain was divided into two parts to reduce the total number of cells and therefore calculation time. The whole area was modelled with a coarser grid and the area upstream the weirs was modelled with finer cells 40% of the size of the original cells (Figure 9) in a first step and 20% of the size in a restart run. That resulted in approximately 2 million cells for the first run and 11 million cells for the second one.

For the time discretization of the turbulent, multiphase flow (water and air) an implicit unsteady model was used with a time step of 0.02 s.

The Reynolds-Averaged Navier Stokes (RANS) equations were solved using the standard k- ϵ model in combination with the SIMPLE method and wall laws at bed and side boundaries.

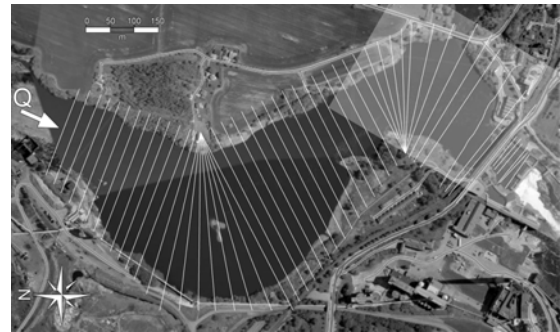


Fig. 9 Project area with cross-sections used for setting up geometry and mesh refinement zone (highlighted).

4.3 Results and discussion

An isosurface has to be defined to visualize the free surface in STAR-CCM+ using the VOF method. The VOF value for that isosurface was set to 0.5 in the current study, which means that the free surface is placed at cells that are 50% filled with water and air.

Figure 10 shows the location of the three cross-sections compared in this study. They are positioned between the bridge piers and the weirs. Figure 11 shows that the overall pattern of the free surface in the area between the bridge and the weirs in the physical model look similar to that of the numerical model.

Figure 12 gives a more detailed impression of the quality of the numerical results. It is clear that the results are quite reasonable. But there are deviations between measurement and simulation in some parts of the cross-sections.

One reason for the deviations is the fact that the surface waves are moving slightly over time and therefore are not exactly at the same position in all three dimensions of space. This makes the measurement of the free surface in that area

difficult. Another possible reason for the deviations is air entrainment. This can be observed in Figure 11 in the area close to the weirs. A third reason for the deviations could be the complexity of the bed topography which could not be captured 100 percent as it is in the physical model.

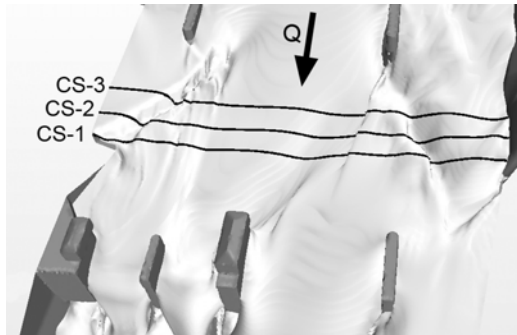


Fig. 10 Location of three free surface measurement cross-sections (CS).

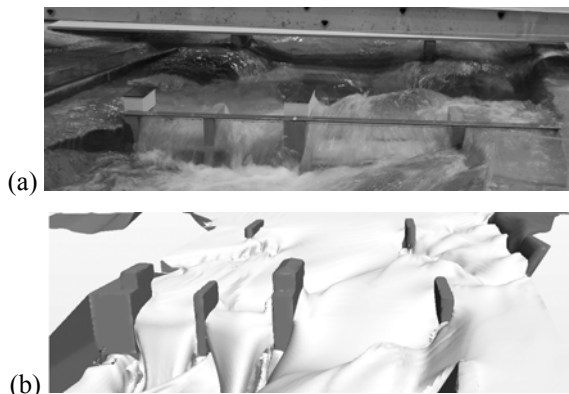


Fig. 11 Free surface comparison, (a) model test and (b) simulation, looking upstream.

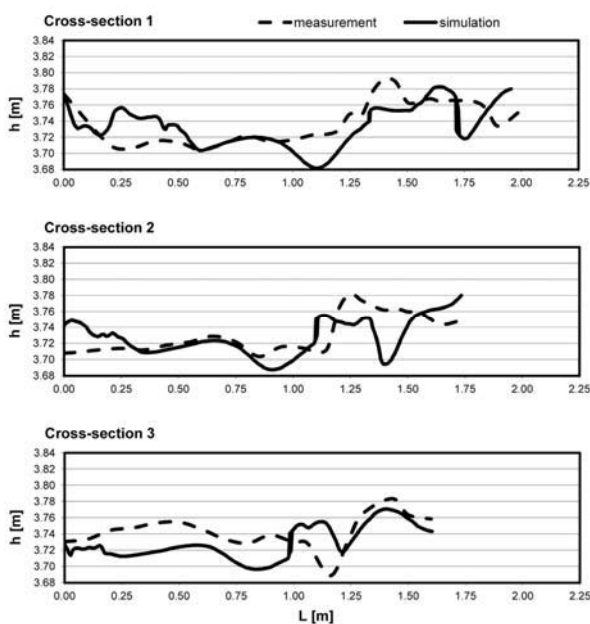


Fig. 12 Free surface comparison in three cross-sections, looking upstream.

5. CONCLUSIONS

Three dimensional numerical simulations have been conducted and the results have been compared with measurements of three physical models with supercritical flow. Two idealized channel geometries from literature have been used for validation: An expansion and a channel junction. The third study was a natural river geometry of the flow situation upstream the weirs of the Sarpfossen dam. The first case shows shock waves along the sides of the expanding channel. At the channel junction, the maximum height of the shock wave is at the side wall downstream the junction. The supercritical flow in the natural river upstream the weir shows several complex oblique standing waves, interacting with each other. All results show that the numerical model (STAR-CCM+) is capable of reproducing the free surface of such flows reasonably well.

When working with the VOF model in STAR-CCM+ it is important to use a time step and a grid cell size small enough to obtain a sharp interface and to avoid false diffusion between the two phases, in this case water and air.

In the future some numerical variations should be tested, to see if it is possible to reduce the small deviations between measurement and simulation. For flows with high Froude numbers the implementation of air entrainment in the numerical model might improve the results. Besides that, different turbulence models (e. g. LES) should be tested.

REFERENCES

1. Bowers CE (1950). *Studies of Open Channel Junctions*. (Part V of Hydraulic model studies for Whiting Field Naval Air Station, Milton, Florida, University of Minnesota, St. Anthony Falls Hydraulic Laboratory) Technical Paper No. 6, Series B.
2. Bürgisser MF (1998). *Numerische Simulation der freien Wasseroberfläche bei Ingenieurbauten*. Doctoral thesis ETH No. 12899, Swiss Federal Institute of Technology, Zurich, Switzerland (in German).
3. Bürgisser MF, Rutschmann P (1999). Numerical solution of viscous 2DV free surface flows: Flow over spillway crests. *Proceedings of 28th IAHR Congress*, Graz, Austria.
4. CD-Adapco (2010). *User Guide STAR-CCM+ Version 5.04.006*.
5. Chan STK, Larock BE (1973). Fluid flows from axisymmetric orifices and valves.

- Journal of the Hydraulics Division ASCE* 99(1):81-97.
6. Chan STK, Larock BE, Herrmann LR (1973). Free-surface ideal fluid flows by finite elements. *Journal of the Hydraulics Division ASCE* 99(6):959-974.
 7. Chandler K, Gill D, Maher B, Macnish S, Roads G (2003). Coping with probable maximum flood – an alliance project delivery for Wivenhoe Dam. *Proceedings of the 43rd ANCOLD Conference*, Hobart, Tasmania, 332–349.
 8. Ferziger JH, Perić M (2002). *Computational Methods for Fluid Dynamics*. 3rd rev. ed. Springer-Verlag, Berlin Heidelberg New York.
 9. Gessler D, Rasmussen B (2005). Before the flood. *Desktop Engineering Magazine*. Available at: <http://www.deskeng.com/article/s/aaabhe.htm> (Accessed 17/03/2011).
 10. Hager WH (1989). Supercritical flow in channel junctions. *Journal of Hydraulic Engineering* 115(5):595-616.
 11. Hargreaves DM, Morvan HP, Wright NG (2007). Validation of the volume of fluid method for free surface calculation: the broad-crested weir. *Engineering Applications of Computational Fluid Mechanics* 1(2):136-146.
 12. Harlow FH, Welch JE (1965). Numerical calculation of time-dependent viscous incompressible flow of fluid with free surface. *The Physics of Fluids* 8(12):2182-2189.
 13. Haun S, Olsen NRB, Feurich R (2011). Numerical modelling of flow over a trapezoidal broad-crested weir. *Engineering Applications of Computational Fluid Mechanics* 5(3):397-405.
 14. Hirt CW, Nichols BD (1981). Volume of fluid (VOF) method for the dynamics of free boundaries. *Journal of Computational Physics* 39:201-225.
 15. Huerta A, Liu WK (1988). Viscous flow with large free surface motion. *Computer Methods in Applied Mechanics and Engineering* 69:277-324.
 16. Hughes TJR, Liu WK, Zimmermann TK (1981). Lagrangian-Eulerian finite element formulation for incompressible viscous flows. *Computer Methods in Applied Mechanics and Engineering* 29:329-349.
 17. Ippen AT, Dawson JH (1951). Design of channel contractions. *Trans. ASCE* 116:326-346.
 18. Ippen AT, Knapp RT (1936). A study of high velocity flow in curved channels. *Trans. American Geophysical Union, Part II* 17:516-521.
 19. Jimenez OF, Chaudhry MH (1988). Computation of supercritical free-surface flows. *Journal of Hydraulic Engineering* 114:377-395.
 20. Krüger S (2000). *Computational Contributions to Highly Supercritical Flows*. Doctoral thesis ETH No.13838, Swiss Federal Institute of Technology, Zurich, Switzerland.
 21. Krüger S, Bürgisser MF, Rutschmann P (1998). Advances in calculating supercritical flows in spillway contractions. In *Hydroinformatics '98*. Ed. Babovic, Larsen. Balkema, Rotterdam, The Netherlands.
 22. Krüger S, Rutschmann P (2006). Modeling 3D supercritical flow with extended shallow-water approach. *Journal of Hydraulic Engineering* 132(9):916-926.
 23. Mazumder SK, Hager WH (1993). Supercritical expansion flow in Rouse modified and reversed transitions. *Journal of Hydraulic Engineering* 119(2):201-219.
 24. Mignot E, Paquier A, Rivière N (2008). Experimental and numerical modelling of symmetrical four-branch supercritical cross junction flow. *Journal of Hydraulic Research* 46(6):723-738.
 25. Mnasri C, Hafsia Z, Omri M, Maalel K (2010). A moving grid model for simulation of free surface behavior induced by horizontal cylinders exit and entry. *Engineering Applications of Computational Fluid Mechanics* 4(2):260-275.
 26. Olsen NRB, Kjellesvig HM (1998). Three-dimensional numerical flow modelling for estimation of spillway capacity. *Journal of Hydraulic Research* 36(5):775-784.
 27. Rouse H, Bhoota BV, Hsu EY (1951). Design of channel expansions. *J. Trans. ASCE* 116:347-363.
 28. Sethian JA (1996). Theory, algorithms, and applications of level set methods for propagating interfaces. *Acta Numerica* 5:309-395.
 29. Soulis JV (1991). A numerical method for subcritical and supercritical open channel flow calculation. *International Journal for Numerical Methods in Fluids* 13(4):437-464.
 30. Stamou I, Chapsas DG, Christodoulou GC (2008). 3-D numerical modeling of supercritical flow in gradual expansions. *Journal of Hydraulic Research* 46(3):402-409.
 31. Ying X, Jorgeson J, Wang SY (2009). Modeling dam-break flows using finite volume method on unstructured grid.

Engineering Applications of Computational Fluid Mechanics 3(2):184-194.

32. Zhou L, Liu D, Ou C (2011). Simulation of flow transients in a water filling pipe containing entrapped air pocket with VOF model. *Engineering Applications of Computational Fluid Mechanics* 5(1):127-140.